Contents

1. An Introduction to the Large Deviation Theory

The Large Deviation Theory was largely developed in 1960s-1970s by S. R. Srinivasa Varadhan, (currently Professor in New York University, Department of Mathematics) in the United States and by Mark Freidlin (also click here) (currently Professor in the University of Maryland, Department of Mathematics) and Alexander Wentzell (currently Professor Emeretus in Tulane University, Department of Mathematics) in the Soviet Union.

The most well-known reference for the Large Deviation Theory is the book by Freidlin and Wentzel [16]. Its first edition appeared in Russian in the late 1970s, its most recent edition is the 3rd edition that appeared in 2013.

In these notes, for simplicity, we will focus on the stochastic differential equation (SDE)

$$(1) \qquad dx = b(x)dt + \sqrt{\epsilon}dw, \quad x \in \mathbb{R}^d$$

where $b(x)$ is a continuously differentiable vector field with a finite number of isolated equilibria, ϵ is a small parameter, and w is the standard Brownian motion.

1.1. **Long-time behavior of solutions of $\dot{x} = b(x)$.** Together with Eq. (1) we also consider the unperturbed deterministic equation

$$(2) \qquad \frac{dx}{dt} = b(x).$$

We assume that the vector field $b(x)$ is such that for any initial condition $x(0) = x_0$ the characteristic of Eq. (2) starting at x_0 will remain in some bounded region. (*A characteristic is the equivalence class of trajectories that can be mapped one to another by a time shift. In other words, a characteristic is a curve on the phase plane depicting a solution of the ODE extended to the maximal time interval.*) In other words, we will consider only such vector fields $b(x)$ that no characteristic goes to infinity at $t \to \infty$.

The solutions of the algebraic equation $b(x) = 0$ are called equilibria or equilibrium points, or stationary points.

Definition 1.   • *An equilibrium x^* is called* stable *if for any its neighborhood $U(x^*)$ one can find a neighborhood $V(x^*) \subset U(x^*)$ such that any characteristic starting in $V(x^*)$ will remain in $U(x^*)$.*
- *Otherwise, the equilibrium is called unstable.*
- *If x^* is a stable equilibrium, and every characteristic $x(t)$ starting in $V(x^*)$ approaches x^* as $t \to \infty$, then the equilibrium x^* is called asymptotically stable.*

We assume that the equation $b(x) = 0$ has a finite number of solutions. This implies, in particular, that all equilibria are isolated.

To summarize, we assume that a vector field in ODE (2) satisfies the following conditions:

A1: $b(s)$ is continuously differentiable,

A2: every characteristic of Eq. (2) remains in a bounded region,

A3: $b(x) = 0$ has at most a finite number of zeros.

The long-time behavior of Eq. (2) with $b(x)$ satisfying the discussed assumptions is simple in 1D. For every initial condition $x(0) = x_0$, the characteristic $x(t)$ tends to some asymptotically stable equilibrium. All equilibrium points are solutions of the algebraic equation $b(x) = 0$.

Now we discuss the long-time behavior of a characteristic in higher dimensions.

Definition 2. *Let $x(t)$ be a characteristic of Eq. (2) staying in a bounded region D. A point x^* is a limit point of $x(t)$ if there exists a sequence of moments of time $\{t_n\} \to \infty$ such that*

$$x(t_n) \to x^* \text{ as } n \to \infty.$$

The set of all limit points of a characteristic $x(t)$ is called the ω-limit set of $x(t)$.

The long-time behavior of Eq. (2) in 2D is more complicated [24]. ω-limit sets of trajectories are always connected and compact. Under assumptions A1, A2, and A3, there are three kinds of possible ω-limit sets in 2D:

(1) an equilibrium point;
(2) a limit cycle (a closed characteristic corresponding to a periodic solution of Eq. (2));

(3) a set consisting of equilibria and characteristics approaching equilibria at $t \to \pm\infty$. These types of ω-limit sets are illustrated in Fig. 1.
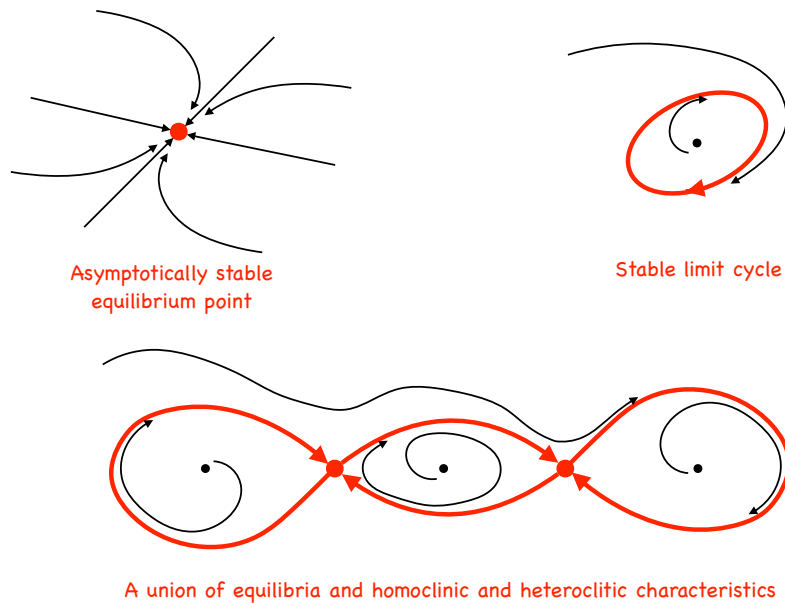

Asymptotically stable
equilibrium point

Stable limit cycle

A union of equilibria and homoclinic and heteroclitic characteristics

FIGURE 1. The three possible types of ω-limit sets of trajectories of ODE (2) in 2D.

ω-limit sets in dimensions three and higher can be very complicated. The most famous example is the Lorenz'63 system where almost all characteristics approach a certain fractal set at appropriate ranges of parameter values [27]. Other such examples are given by the Roessler system [31] and Gissinger's model for chaotic reversals [19].

The term *attractor* is commonly used when the long-time behavior of solutions of autonomous ODEs is discussed. This term is hard to define rigorously. On one hand, the definition should be broad enough to embrace all known candidates. On the other hand, it should exclude impostors. Below is the definition given in S. Strogatz's book [34]

Definition 3. *An attractor is a closed set A possessing the following properties:*

(1) *A is an invariant set, i.e., any trajectory starting in A remains in A for all time.*

(2) *A attracts an open set of initial conditions: there is an open set $U \supset A$ such that for all trajectories with $x(0) \in U$, the distance between $x(t)$ and A tends to zero at $t \to \infty$. The maximal set U with this property is called the basin of attraction of A.*

    (3) *A is minimal, i.e., there is no proper subset of A that satisfies properties (1) and (2).*

In summary, any characteristic of ODE (2) provided that assumptions A1, A2, and A3 hold, approaches some attractor as $t \to \infty$.

The long-time behavior of SDE (1) is much more complicated. No matter how small the noise term is, trajectories of SDE (1) will escape from any neighborhood of any attractor of the corresponding ODE if you wait long enough. If the ODE has multiple attractors, the noise term in the corresponding SDE enables transitions between them. The large deviation theory [16] quantifies escapes from neighborhoods of attractors and transitions between various attractors, i.e., gives asymptotic estimates for escape times and escape paths. In the next few sections, we will discuss the key concepts of the large deviation theory in terms of which the aforementioned estimates are given. Then we will discuss numerical tools for finding these estimates.

1.2. **Freidlin-Wentzell Action Functional.** Let x_0 and x_1 be two points in $\mathbb{R}^d$. We consider a set of all absolutely continuous paths $\phi : [0, T] \to \mathbb{R}^d$ connecting x_0 and x_1. The Freidlin-Wentzell action functional $S_T(\phi)$ is defined by

$$(3) \qquad S_T(\phi) = \frac{1}{2} \int_0^T \|\dot\phi - b(\phi(t))\|^2 dt, \quad \phi(0) = x_0, \quad \phi(T) = x_1,$$

where $\|\cdot\|$ is the two-norm, $\dot\phi \equiv \frac{d\phi}{dt}$. If $\phi(t)$ is a solution of $\dot x = b(x)$, i.e., then the Freidlin-Wentzel action along this path is zero. Otherwise it is positive. Let us give an insight of where the Freidlin-Wentzell action comes from. The reasoning below is far from rigorous. An interested reader should study Ref. [16].

Consider a solution $x(t)$ of Eq. (1). Let us calculate the probability that $x(t)$ nearly follows a given path $\phi(t)$. Motivated by the fact that

$$dx - b(x)dt = \sqrt{\epsilon}dw$$

we define another path $\xi(t)$ that should be followed by the Brownian motion:

$$d\xi(t) = (\dot\phi - b(\phi))dt, \quad \xi(t) = \int_0^t (\dot\phi - b(\phi))d\tau.$$

If the solution $x(t)$ stays close to $\phi(t)$, then the scaled Brownian motion $\sqrt{\epsilon}w(t)$ should stay close to the path $\xi(t)$. Now we outline the calculation of the probability that j-th component of the scaled Brownian motion $\sqrt{\epsilon}w(t)$ stays in the ϵ-tube surrounding the j-th component of the path $\xi(t)$. This can be done using the Wiener measure as follows. We discretize the time interval $[0, T]$

$$0 < t_1 < t_2 < \ldots < t_n = T$$

so that the length of each subinterval is h. Recall that $\sqrt{\epsilon}(w(t + h) - w(t)) \sim N(0, \epsilon h)$. Then the probability that each component $\sqrt{\epsilon}w_j(t)$ stays within distance ϵ of $\xi_j(t)$ is given

by

$$P(\max_{1\leq j\leq d}\max_{0\leq t_k\leq T}|\sqrt{\epsilon}w_j(t_k)-\xi_j(t_k)|<\delta)$$

$$=\prod_{j=1}^{n}\lim_{n\to\infty}\int_{\xi_j(t_1)-\delta}^{\xi_j(t_1)+\delta}\frac{e^{-(y_1-\xi_j(0))^2/2\epsilon h}}{\sqrt{2\pi\epsilon h}}dy_1\int_{\xi_j(t_2)-\delta}^{\xi_j(t_2)+\delta}\frac{e^{-(y_2-y_1)^2/2\epsilon h}}{\sqrt{2\pi\epsilon h}}dy_2$$

(4)
$$\cdots\int_{\xi_j(t_n)-\delta}^{\xi_j(t_n)+\delta}\frac{e^{-(y_n-y_{n-1})^2/2\epsilon h}}{\sqrt{2\pi\epsilon h}}dy_n.$$

For any $1\leq k\leq n$, one can make a variable change $y_k=\xi_k(k)+u_k$. Then

$$\int_{\xi_j(t_k)-\delta}^{\xi_j(t_k)+\delta}\frac{e^{-\frac{(y_k-y_{k-1})^2}{2\epsilon h}}}{\sqrt{2\pi\epsilon h}}dy_k=\int_{-\delta}^{\delta}\frac{e^{-\frac{(\xi_j(t_k)-y_{k-1}+u_k)^2}{2\epsilon h}}}{\sqrt{2\pi\epsilon h}}du_k.$$

Note that

$$\frac{(\xi_j(t_k)-\xi_j(t_{k-1}))^2}{2\epsilon h}=\frac{(\dot{\phi}_j-b_j(\phi(t)))^2h^2}{2\epsilon h}=\frac{1}{2\epsilon}(\dot{\phi}_j-b_j(\phi(t)))^2h.$$

Pulling these terms outside each sub-integral, carefully taking the limits: first $n\to\infty$, then $\delta\to 0$, and and finally $\epsilon\to 0$, one obtains that

(5) $$P(\|\sqrt{\epsilon}w_t-\xi(t)\|_{\max}<\delta)\asymp\exp\left\{-\frac{1}{2\epsilon}\int_0^T\|\dot{\phi}-b(\phi(t))\|^2dt\right\}\equiv\exp\left\{-\frac{S_T(\phi)}{\epsilon}\right\},$$

where S_T is the Freidlin-Wentzel action Eq. (3). The symbol '$\asymp$' denotes logarithmic equivalence. Eq. (5) means that

(6) $$-\lim_{\epsilon\to 0}\epsilon\log\left[P(\|\sqrt{\epsilon}w_t-\xi(t)\|_{\max}<\delta)\right]=S_T(\phi),$$

i.e.,

$$P(\|\sqrt{\epsilon}w_t-\xi(t)\|_{\max}<\delta)=g(\epsilon,\phi,\delta)\exp\left\{-\frac{S_T(\phi)}{\epsilon}\right\},$$

where the function $g(\epsilon,\cdot)$ called a *prefactor* is such that it decays to zero as $\epsilon\to 0$ so that

$$\lim_{\epsilon\to 0}\epsilon\log g(\epsilon,\cdot)=0.$$

The Freidlin-Wentzell theory is concerned only with asymptotic estimates up to exponential orders. Most of its results have the form of Eq. (6).

1.3. **The quasipotential.** Now we consider the problem of exiting from a region D surrounding an attractor. The expected exit times and the transition rates are defined in terms of the *quasipotential*. We start with the simplest case where the attractor is an asymptotically stable equilibrium x_0 of $\dot{x}=b(x)$. The quasipotential $U_{x_0}(x)$ at point x with respect to the point x_0 is defined as the infimum of the Freidlin-Wentzell action over all possible times T and all absolutely continuous paths ϕ connecting the points x_0 and x:

(7) $$U_{x_0}(x)=\inf_{\phi,T}\left\{S_T(\phi)\,|\,\phi(0)=x_0,\ \phi(T)=x\right\}.$$

The expected exit time $\mathbb{E}[\tau_{exit}]$ from the basin of attraction $B(x_0)$ of the point x_0 is logarithmically equivalent to [16]

$$\mathbb{E}[\tau_{exit}] \asymp e^{\frac{1}{\epsilon} \min_{x \in \partial B(x_0)} U_{x_0}(x)}. \tag{8}$$

Moreover, the maximum likelihood exit path from $B(x_0)$ is the minimizer of the Freidlin-Wentzell action over all absolutely continuous paths from the point x_0 to the boundary of its basin of attraction and all times T. Such a path is called the *Minimum Action Path (MAP)* or the *instanton*. A sharp estimate (including a prefactor) for the expected exit time from the basin of an asymptotically stable equilibrium via a saddle point with only one unstable direction provided that the quasipotential is smooth near the saddle is given by Bouchet and Reygner in [4].

1.4. **The geometric action.** The infimum in time in Eq. (7) can be taken analytically. Let a point x_0 be an asymptotically stable equilibrium of $\dot{x} = b(x)$, and a point x belong to its basin of attraction. The minimization with respect to the travel-time T can be performed analytically [16, 23, 22] resulting at the geometric action $S(\psi)$. Let $\phi(t)$ be a fixed absolutely continuous path $\phi(t)$. Expanding $\|\cdot\|^2$ in Eq. (3) and using the inequality $y^2 + z^2 \geq 2yz$ for all nonnegative real numbers y and z, we get:

$$\begin{aligned}
S_T(\phi) = \frac{1}{2} \int_0^T \|\dot{\phi} - b(\phi)\|^2 dt &= \frac{1}{2} \int_0^T \left(\|\dot{\phi}\|^2 - 2\dot{\phi} \cdot b(\phi) + \|b(\phi)\|^2 \right) dt \\
&\geq \frac{1}{2} \int_0^T \left(2\|\dot{\phi}\|\|b(\phi)\| - 2\dot{\phi} \cdot b(\phi) \right) dt \\
&= \int_0^T \left(\|\dot{\phi}\|\|b(\phi)\| - \dot{\phi} \cdot b(\phi) \right) dt.
\end{aligned} \tag{9}$$

The inequality in Eq. (9) becomes an equality if and only if $\|\dot{\phi}\| = \|b(\phi)\|$. The last integral is independent of the parametrization of the path ϕ. Let χ be the path obtained from ϕ by a reparametrization such that $\|\dot{\chi}\| = \|b(\chi)\|$. Then

$$S_T(\phi) \geq S_{T_\chi}(\chi) = \int_0^{T_\chi} (\|\dot{\chi}\|\|b(\chi)\| - \dot{\chi} \cdot b(\chi)) \, dt. \tag{10}$$

Note that T_χ can be infinite. The integral in right-hand side of Eq. (10) is invariant with respect to the parametrization of the path χ. Hence, we can pick the most convenient one, for example, the arclength parametrization, and denote the reparametrized path by ψ. Hence,

$$S_{T_\chi}(\chi) = \int_0^L (\|\psi_s(s)\|\|b(\psi(s))\| - \psi_s(s) \cdot b(\psi(s))) \, ds =: S(\psi), \tag{11}$$

where L is the length of the paths χ and ψ (corresponding to the same curve). For computation of the quasi-potential, it is more convenient to deal with the geometric action $S(\psi)$ than with the Freidlin-Wentzell action $S_T(\phi)$.

We note that the value of integral in Eq. (11) is independent of the choice of parametrization of the path ψ. We mostly will use either the arclength parametrization or the uniform parametrization on the interval $[0, 1]$. Then the geometric action becomes

$$(12) \qquad S(\psi) = \int_0^L \{\|b(\psi(s)\|\|\psi_s\| - b(\psi(s)) \cdot \psi_s\} \, ds$$

for the arclength parametrization, where L is the length of the path, and

$$(13) \qquad S(\psi) = \int_0^1 \{\|b(\psi(\alpha))\|\|\psi_\alpha\| - b(\psi(\alpha)) \cdot \psi_\alpha\} \, d\alpha$$

for the uniform parametrization on the interval $[0, 1]$.

1.5. **The case of the overdamped Langevin dynamics.** Consider the overdamped Langevin dynamics:

$$(14) \qquad dx = -\nabla V(x) dt + \sqrt{2\beta^{-1}} dw,$$

where $\beta = (k_B T)^{-1}$, k_B is the Boltzmann constant, T is the absolute temperature. Then the minimum and the minimizer of the geometric action have a simple characterization [22]. Suppose a path $\psi(s)$ connects two local minima x_A and x_B of $V(x)$ separated by a single saddle x_{AB}. Consider first the part of the path going uphill and set

$$\psi(0) = x_A, \quad \psi(1) = x_{AB}.$$

Start from Eq. (13) and replace $b(c)$ with $-\nabla V(x)$ in it:

$$S(\psi) = \int_0^1 \{\|\nabla V(\psi(\alpha))\|\|\psi_\alpha\| + \nabla V(\psi(\alpha)) \cdot \psi_\alpha\} \, d\alpha$$

$$= \int_0^1 \{\|\nabla V(\psi(\alpha))\|\|\psi_\alpha\|\} \, d\alpha + V(x_{AB}) - V(x_A).$$

Note that

$$\|\nabla V(\psi(\alpha))\|\|\psi_\alpha\| \geq \nabla V(\phi) \cdot \phi_\alpha,$$

and the equality takes place if and only if ϕ_α is parallel to $\nabla V(\phi(\alpha))$. Hence

$$S(\psi) \geq \int_0^1 \nabla V(\psi(\alpha)) \cdot \psi_\alpha d\alpha + V(x_{AB}) - V(x_A) = 2(V(x_{AB}) - V(x_A)).$$

Therefore, the quasipotential with respect to a minimum x_A within its basin of attraction is the doubled potential. Note that traveling along the steepest descent path $\dot\phi = -\nabla V(\phi)$ from the saddle x_{AB} to the minimum does not contribute to the geometric action.

The result that $\min_\psi S(\psi) = 2(V(x_{AB}) - V(x_A))$ where the minimum is taken over all paths starting at the local minimum x_A and ending at the local minimum x_B, is consistent with the Arrhenius law. Indeed, the transition rate from x_A to x_B, which is the reciprocal of the expected exit time from the basin of attraction of x_A is

$$r_{AB} \asymp \exp\left\{-\frac{\beta}{2} 2(V(x_{AB}) - V(x_A))\right\} = \exp\{-\beta(V(x_{AB}) - V(x_A))\}.$$

The path ψ that minimizes the geometric action is the one satisfying the condition $\frac{d\psi}{d\alpha}$ is parallel to $\nabla V(\psi)$, i.e., the velocity vector of the path is parallel to the gradient of the vector field. Hence, the path ψ goes either *directly uphill or directly downhill*. A path ψ going directly uphill or directly downhill is called the *Minimum Energy Path* or *MEP*. The collection of MEPs connecting every pair of neighboring minima in the 7-well potential is shown in Fig. 2.
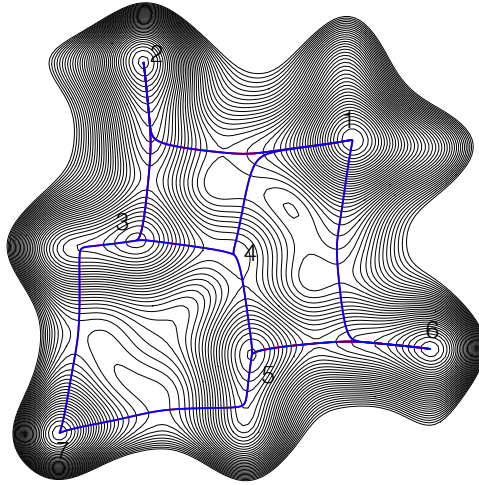

FIGURE 2. The Minimum Energy Paths (MEPs) connecting every pair of neighboring minima in the 7-well potential.

1.6. **Quasipotential with respect to compact sets.** In order to define the quasipotential with respect to more complex attractors than asymptotically stable equilibria, we extend its definition to a function defined on pairs of compact sets in $\mathbb{R}^n$.

Definition 4. *For any pair of compact sets $X_0 \subset \mathbb{R}^n$ and $X \subset \mathbb{R}^n$ we define the quasipotential as*

$$(15) \qquad U(X_0, X) = \inf \left\{ S(\psi) \,|\, \psi(0) \in X_0, \; \psi(1) \in X \right\}.$$

It follows from Eqs. (12) and (15) that the quasipotential is Lipschitz-continuous function with respect to both of its arguments on every compact set D, and the Lipschitz constant is $2 \max_D |b|$. If X_0 and X are points then

$$|U(X_0, X) - U(Y_0, Y)| \leq 2 \max_D \|b\| \left(\|X_0 - Y_0\| + \|X - Y\| \right).$$

If X_0 and X are compact sets, the same is true with respect to the Hausdorff distance.

An important property of the quasipotential is that it is constant on every attractor of the system. This property is summarized in the following theorem [5]

Theorem 1. *Let X_0 be a compact set. Let $C = \{z(t) \,|\, t \geq 0\}$ be a trajectory of $\dot{x} = b(x)$, and F be its ω-limit set. Then*

(1) $U(X_0, y) = U(X_0, F)$ *for all $y \in F$, i.e, the quasipotential $U(X_0, y)$ is constant on the ω-limit set F and equals to $U(X_0, F)$.*

(2) $U(y, X_0) = U(F, X_0)$ *for all $y \in F$, i.e, the quasipotential $U(y, X_0)$ is constant on the ω-limit set F and equals to $U(F, X_0)$.*

1.7. **The Hamilton-Jacobi-Bellman equation for the quasipotential.** In this section, we derive the Hamilton-Jacobi-Bellman equation for the quasipotential from the Bellman Principle of Optimality [3]. This equation will provide us with the relationship between the velocity vector ψ_s of the *Minimum Action Path* (MAP) (i.e., the minimizer of the geometric action) and the gradient of the quasipotential that will enable us to compute the MAP once we have found the quasipotential.

Let us fix some compact set X_0 and consider the quasipotential $U(x) \equiv U(X_0, x)$ as a function of the point x. Then the function $U(x)$ is given by

$$(16) \qquad U(x) = \left\{ \inf_{\psi, L} \int_0^L \left\{ \|b(\psi(s)\|\|\psi_s\| - b(\psi(s)) \cdot \psi_s \right\} ds \,\middle|\, \psi(0) \in X_0, \ \psi(L) = x \right\}.$$

Bellman's Principle of Optimality: *An optimal policy has the property that whatever the initial state and initial decision are, the remaining decisions must constitute an optimal policy with regard to the state resulting from the first decision.*

We will treat the quasipotential $U(x)$ as the value function, the integrand in Eq. (16) as the cost function, and unit velocity vector ψ_s as the control. The Bellman optimality principle reads

$$(17) \qquad U(x) = \inf_{\psi_s(s)} \left\{ \int_0^l (\|b(\psi(s))\| - b(\psi(s)) \cdot \psi_s) ds + U\left(x - \int_0^l \psi_s(s) ds\right) \right\}.$$

We fix a small $\epsilon > 0$ and set $l = \epsilon$. Then Eq. (17) becomes

$$(18) \qquad U(x) = \inf_{\psi_s \in \mathbb{S}^{n-1}} \left\{ (\|b(\psi)\| - b(\psi) \cdot \psi_s)\epsilon + U(x) - (\nabla U(x) \cdot \psi_s)\epsilon + O(\epsilon^2) \right\},$$

where $\mathbb{S}^{n-1}$ is the unit sphere in $\mathbb{R}^n$. Canceling $U(x)$, dividing by ϵ, and taking the limit $\epsilon \to 0$, we obtain the static Hamilton-Jacobi-Bellman equation

$$(19) \qquad H(x, \nabla U) := \inf_{\psi_s \in \mathbb{S}^{n-1}} \left\{ \|b(x)\| - (b(x) + \nabla U(x)) \cdot \psi_s \right\} = 0.$$

The control $\psi_s \in \mathbb{S}^{n-1}$ that gives the infimum in Eq. (19) can be found explicitly. We observe that

$$-\|b + \nabla U\| \leq (b + \nabla U) \cdot \psi_s \leq \|b + \nabla U\|.$$

Therefore, the infimum is achieved if

$$\psi_s = \frac{b + \nabla U}{\|b + \nabla U\|}.$$

Furthermore, this infimum equals zero if and only if $\|b + \nabla U\| = \|b\|$. Hence the optimal control ψ_s and the gradient of the value function ∇U are related via

$$(20) \qquad \boxed{\psi_s = \frac{b + \nabla U}{\|b\|}, \quad \nabla U = \|b\|\psi_s - b.}$$

The equation $\|b + \nabla U\| = \|b\|$ implies that

$$(21) \qquad \boxed{\|\nabla U\|^2 + 2\nabla U \cdot b(x) = 0, \quad U|_{X_0} = 0.}$$

We will refer to Eq. (21) as the Hamilton-Jacobi equation for the quasipotential.

Note that

$$\|\nabla U\|^2 + 2\nabla U \cdot b(x) = \nabla U \cdot (\nabla U + 2b(x)) = 0.$$

The last equality shows that $\nabla U(x)$ belongs to the sphere of radius $\|b(x)\|$ centered at $b(x)$ as shown in Fig. 3, and the direction of the MAP ψ_s at a point x is collinear to $b(x) + \nabla U(x)$.
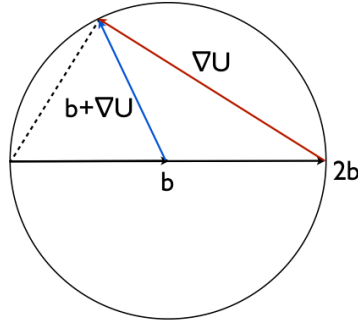

FIGURE 3. The relationship between the force field $b(x)$, the gradient of the quasipotential $\nabla U(x)$, and the direction of the Minimum Action path $\psi_s \parallel b + \nabla U$.

The Hamilton-Jacobi-Bellman equation (21) implies that the vector field $b(x)$ can be decomposed into the potential component and the orthogonal to it rotational component wherever $U(x)$ is continuously differentiable as

$$(22) \qquad b(x) = -\tfrac{1}{2}\nabla U(x) + \left(\tfrac{1}{2}\nabla U(x) + b(x)\right) \equiv -\tfrac{1}{2}\nabla U(x) + l(x).$$

The orthogonality of $\nabla U(x)$ and $l(x)$ can be shown from Eq. (21) by rewriting it as

$$0 = 2\nabla U \cdot (\tfrac{1}{2}\nabla U + b(x)) = 2\nabla U \cdot l(x).$$

Eq. (20) implies that the *Minimum Action Paths* (MAPs) are the flowlines of the field $\tfrac{1}{2}\nabla U + l(x)$, i.e., *the MAPs follow the rotational component of the field but go against its potential component* as in an example provided in [16] (Chapter 4, Theorem 3.1, p. 118).

I would like to emphasize that the Hamilton-Jacobi equation (21) with the boundary condition $U(x) = 0$ at a given attractor does **not** define the quasipotential. The quasipotential is just one of its solutions. Generally, it is a so called viscosity solution as the quasipotential might be non-differentiable. There is always at least one more solution $U(x) = 0$ for all x.

There can be other nontrivial solutions of Eq. (21) besides the quasipotential. Let us demonstrate this phenomenon on an example.

Example 1   One can check that the quasipotential for the 2D linear SDE

$$(23) \qquad dx = Axdt + \sqrt{\epsilon}dw, \quad A = \begin{bmatrix} -1 & -1 \\ 0 & -1 \end{bmatrix}$$

is given by

$$(24) \qquad U(x) = \frac{1}{5}\left(4x_1^2 + 4x_1x_2 + 6x_2^2\right).$$

This solution is found using formula (31) below. Therefore, the potential and rotational components of the vector field Ax are given by $-Qx \equiv -\frac{1}{2}\nabla U(x)$ and Lx respectively where the matrices Q and L are

$$(25) \qquad Q = \frac{1}{5}\begin{bmatrix} 4 & 2 \\ 2 & 6 \end{bmatrix}, \quad L = \frac{1}{5}\begin{bmatrix} -1 & -3 \\ 2 & 1 \end{bmatrix}.$$

It is easy to check that the $U(x)$ satisfies the Hamilton-Jacobi equation (21). Canceling the factor of 4 we get:

$$x^\top Q\left(Q + A\right)x^\top = 0 \quad \text{for all} \ \ x$$

as the matrix $Q(Q + A)$ is antisymmetric, indeed:

$$Q(Q + A) = \frac{1}{25}\begin{bmatrix} 4 & 2 \\ 2 & 6 \end{bmatrix}\begin{bmatrix} -1 & -3 \\ 2 & 1 \end{bmatrix} = \frac{1}{5}\begin{bmatrix} 0 & -2 \\ 2 & 0 \end{bmatrix}.$$

On the other hand, let us consider the decomposition $A = -V + R$ where

$$V = \begin{bmatrix} 0 & 0 \\ 0 & 1 \end{bmatrix}, \quad R = \begin{bmatrix} -1 & -1 \\ 0 & 0 \end{bmatrix}$$

It is easy to check that $Vx = -\frac{1}{2}\nabla U_1(x)$ for $U_1(x) = x_2^2$ and that the matrix $V(V + A)$ is zero, hence antisymmetric. Therefore, $U_1(x)$ satisfies the Hamilton-Jacobi equation (21). Hence, we have found another nontrivial solution of (21) that is not the quasipotential.

1.8. **Invariant probability measure.** The quasipotential allows us to estimate the invariant probability measure $m(x)$ in a sublevel set D of the quasipotential with respect to an attractor A

$$D := \{x \in \mathbb{R}^n \mid U_A(x) < a\}$$

such that A is the unique attractor within D [16] (Chapter 4, Theorem 4.3):

$$m(x) \asymp e^{-U_A(x)/\epsilon}.$$

We remind that the symbol $\asymp$ means logarithmic equivalence. Hence this estimate gives the exponent of the equilibrium density but not its prefactor. Let us fix the attractor A of $\dot{x} = b(x)$ and show that

$$(26) \qquad m(x) = Z^{-1} e^{-U(x)/\epsilon},$$

whenever the quasipotential $U(x)$ is continuously differentiable and the rotational component $l(x)$ of the vector field $b(x)$ is divergence-free, i.e., $\nabla \cdot l(x) = 0$.

We remind that a function $m(x)$ is the invariant pdf for SDE (1) if and only if it satisfies the condition $\int_{\mathbb{R}^n} m(x) dx = 1$ and the stationary forward Kolmogorov (a.k.a. the Fokker-Planck) equation

$$-\nabla \cdot (b(x) m(x)) + \tfrac{\epsilon}{2} \Delta m(x) = 0.$$

The last equation can be rewritten as

$$(27) \qquad -\nabla \cdot J(x) = 0, \text{ where } J := J(x) = b(x) m(x) - \tfrac{\epsilon}{2} \nabla m(x)$$

is the probability current.

Suppose the quasipotential $U(x)$ is continuously differentiable. Plugging Eq. (26) into the expression for the probability current $J(x)$ and using the decomposition $b(x) = -\tfrac{1}{2} \nabla U(x) + l(x)$ we get

$$\begin{aligned} J(x) &= b(x) m(x) - \tfrac{\epsilon}{2} \nabla m(x) \\ &= \left(-\tfrac{1}{2} \nabla U(x) + l(x) \right) m(x) + \tfrac{1}{2} \nabla U(x) m(x) = l(x) m(x). \end{aligned}$$

Then its divergence is

$$(28) \qquad \nabla \cdot J(x) = \left(\nabla \cdot l(x) - \epsilon^{-1} l(x) \cdot \nabla U(x) \right) m(x) = m(x) \nabla \cdot l(x)$$

due to the orthogonality of $l(x)$ and $\nabla U(x)$. Therefore, $\nabla \cdot J(x) = 0$ for $m(x)$ given by Eq. (26) if $U(x)$ is continuously differentiable and $l(x)$ is divergence-free.

2. Special cases where the quasipotential can be found analytically

In general, the quasipotential cannot be found analytically. The first numerical solver for the quasipotential for 2D SDEs of the form (1) was proposed in [5] in 2012. This solver was based on the Sethian's and Vladimirsky's Ordered Upwind Method for solving stationary Hamilton-Jacobi equations [32, 33]. A family of more efficient 2D quasipotential solvers named the Ordered Line Integral Methods (OLIMs) was introduced in 2017 in [8]. The OLIMs were extended to the case of variable and anisotropic diffusion in [9]. The OLIMs were promoted to 3D and highly optimized in [39].

Nevertheless, the examples where the quasipotential can be found analytically are very important as they can be used for obtaining asymptotic estimates (this is useful, e.g. for initialization of numerical methods) as well as for testing numerical methods.

2.1. **Periodic trajectories.** It was proven in [5] that the quasipotential with respect to a stable equilibrium surrounded by cyclic characteristics is zero in the region consisting of these characteristics. This is the case, e.g., in the Lotka-Volterra system perturbed by $\sqrt{\epsilon}dw$.

Theorem 2. *Let x_0 be an equilibrium of $\dot{x} = b(x)$, $x \in \mathbb{R}^2$ and all of trajectories in some neighborhood D of x_0 containing no other critical points are periodic. Then $U(x, y) = 0$ for all $x \in D$, $y \in D$.*

2.2. **Linear SDEs.** Let us consider a linear SDE of the form

$$(29) \qquad dx = Axdt + \sqrt{\epsilon}dw, \quad x \in \mathbb{R}^d,$$

where A is such that all of its eigenvalues have negative real parts. Then the origin is an asymptotically stable equilibrium and the only attractor of the system. The quasipotential with respect to it is given by the Chen-Freidlin formula [11, 12]:

$$(30) \qquad U(x) = \frac{1}{2}x^{\top} \left(\int_0^{\infty} e^{At}e^{A^{\top}t}dt \right)^{-1} x.$$

It is shown in [11, 12] that the matrix in Eq. (30) is positive definite. The derivation of Eq. (30) is based on the theorem stating that if all eigenvalues of a matrix A have negative real parts then the matrix equation $AX + XA^{\top} = Y$ has a unique solution for every Y, and this solution is given by $X = \int_0^{\infty} e^{At}(-Y)e^{A^{\top}t}dt$ [20]. Eq. (30) is important from the theoretical point of view. It proves the existence of the quasi-potential decomposition for linear SDEs (29). The uniqueness of this decomposition follows from Theorem 3.1, Section 4.3 in [16]. This theorem says that a continuously differentiable solution $u(x)$ of the Hamilton-Jacobi equation (21) with the boundary condition $u(x) = 0$ on an attractor $\mathcal{A}$ of $\dot{x} = b(x)$ such that $u(x) > 0$ for $x \notin \mathcal{A}$ is the quasi-potential.

While formula (30) is compact and universal, it is not convenient for numerical evaluation.

A different, simple-to-evaluate formula for the quasi-potential for a 2×2 matrix $A = (A_{ij})_{i,j=1,2}$ with all eigenvalues having negative real parts was developed in [5] from geometric considerations:

$$(31) \qquad U(x) = x^{\top} \begin{bmatrix} \mathcal{A} & \mathcal{B} \\ \mathcal{B} & \mathcal{C} \end{bmatrix} x, \quad \text{where}$$

$$\mathcal{A} = -(\alpha A_{11} + \beta A_{21}), \quad \mathcal{B} = -(\alpha A_{12} + \beta A_{22}), \quad \mathcal{C} = -(\alpha A_{22} - \beta A_{12}),$$

$$\alpha = \frac{(A_{11} + A_{22})^2}{(A_{11} + A_{22})^2 + (A_{21} - A_{12})^2}, \quad \beta = \frac{(A_{21} - A_{12})(A_{11} + A_{22})}{(A_{11} + A_{22})^2 + (A_{21} - A_{12})^2}.$$

In dimensions higher than 2, the quasipotential for linear SDEs (29) with an attractor at the origin can be found algorithmically. Eq. (30) shows that the quasipotential is a quadratic form

$$U(x) = x^{\top}Qx$$

where Q is a symmetric positive definite matrix that needs to be found. We will call Q the *quasipotential matrix*. Plugging the gradient $\nabla U(x) = 2Qx$ to the Hamilton-Jacobi equation (21) and canceling the factor of 4 we obtain

$$(32) \qquad x^\top Q (Q + A) x = 0 \quad \text{for all} \quad x \in \mathbb{R}^d.$$

Hence the matrix $Q(Q + A)$ must be antisymmetric, i.e.

$$(33) \qquad Q(Q + A) + (Q + A^\top)Q = QA + A^\top Q + 2Q^2 = 0.$$

Multiplying (33) by Q^{-1} on the left and on the right, we obtain the Sylvester equation (a.k.a. the Lyapunov equation) with respect to Q^{-1}:

$$(34) \qquad AQ^{-1} + Q^{-1}A^\top = -2I.$$

Eq. (34) can be solved is solved by the Bartels-Stewart algorithm [2] that is implemented in MATLAB in the command `sylvester`. Therefore, the quasipotential matrix Q can be calculated in MATLAB using the following command[1]:

```
Q = inv(sylvester(A,A',-2*eye(size(A))))
```

An algorithm for finding the quasipotential for linear SDEs similar to Bartels-Stewart is described in [6].

For linear SDEs (29) the rotational component $l(x) = (A+Q)x =: Rx$ is divergence-free. Indeed,

$$\nabla \cdot Rx = \text{tr}(R) = 0,$$

(see Theorem 5.1 in [6]). Hence, the invariant pdf is given by

$$(35) \qquad m(x) = \frac{\sqrt{\det Q}}{\pi^{d/2} \epsilon^{d/2}} e^{-x^\top Qx/\epsilon}.$$

2.3. **An example with a limit cycle.** We would like to give an example of an equation with a stable limit cycle where the quasipotential can be found analytically. We consider the SDE made up from an example of a system with a stable limit cycle from [24]

$$(36) \qquad dx = (y + x(1 - x^2 - y^2))dt + \sqrt{\epsilon}dw_1$$
$$dy = (-x + y(1 - x^2 - y^2))dt + \sqrt{\epsilon}dw_2.$$

The corresponding equation without the stochastic term takes the form

$$\frac{dr}{dt} = r(1 - r^2), \quad \frac{d\phi}{dt} = -1$$

in the polar coordinates, and its general solution is

$$r(t) = \frac{1}{\sqrt{1 + ke^{-2t}}}, \quad \phi(t) = -(t - t_0),$$

where k and t_0 are arbitrary constants. One can see that this equation has the stable limit cycle $r(t) = 1$ for $k = 0$, and all other trajectories approach it from inside or from outside

---

[1]I thank Prof. Daniel Szyld for pointing out this simple way to find the quasipotential decomposition for linear SDEs using MATLAB.

as $t \to +\infty$. It is easy to decompose the vector field in Eq. (36) into the potential and rotational components

$$b(x, y) = -\tfrac{1}{2}\nabla U + l(x, y)$$

just by glance. One can check that

(37)
$$U = \frac{1}{2}\left(x^4 + 2x^2y^2 + y^4\right) - x^2 - y^2 + \frac{1}{2} = \frac{1}{2}\left(r^2 - 1\right)^2,$$

(38)
$$l = \begin{pmatrix} y \\ -x \end{pmatrix}.$$

One can see from Eq. (37) that the quasipotential $U(r)$ has a minimum at the limit cycle $r = 1$ as $U'(r) = 2r\left(r^2 - 1\right)$ is zero at $r = 1$, and $U''(r) = 6r^2 - 2$ is $4 > 0$ at $r = 1$. Furthermore, we can calculate the angle $\theta(x, y)$ between the vector fields $b(x, y)$ and $l(x, y)$:

$$\cos\theta = \frac{b \cdot l}{|b||l|} = \frac{x^2 + y^2}{r\sqrt{r^6 - 2r^4 + 2r^2}} = \frac{1}{\sqrt{(r^2 - 1)^2 + 1}}.$$

Therefore, θ depends only on r and $\theta(r) \to \arccos(1) = 0$ as $r \to 1$.

The invariant pdf for the diffusion process given by Eq. (36) can be found exactly by

(39)
$$m(x, y) = Z^{-1}e^{-U(x,y)/\epsilon},$$

where $U(x, y)$ is given by Eq. (37) and Z is the normalization constant. Indeed, we have shown in Section 1.8 that it suffices to check whether the rotational component $l(x, y)$ given by Eq. (38) is divergence-free. Obviously, this is the case.

3. Methods for finding Minimum Energy Paths

In this section, we consider systems evolving according to the overdamped Langevin dynamics

$$dx = -\nabla V(x)dt + \sqrt{2\beta^{-1}}dw.$$

The attractors of the corresponding ODE $\dot{x} = -\nabla V(x)$ are local minima of $V(x)$. The maximum likelihood transition paths between them are the so-called Minimum Energy Paths (MEPs) that are parallel to ∇V, i.e., they climb up to saddles along ∇V and descend from saddles along $-\nabla V$. The two most successful methods for finding MEPs are the *nudged elastic band method* (NEB) proposed by Jonsson, Mills, and Jacobsen in 1998 [25] and the *string method* proposed by E, Ren, and Vanden-Eijnden in 2002 [13]. The NEB and the string methods are based on the same curve evolution law stated in Eq. (40) below, but realize it via different numerical implementations. In both cases, the path between minima x_A and x_B is represented by a finite collection of points called *images*. At each step, both methods let the images move along the component of $-\nabla V$ normal to the current path. Then the string method reparametrizes the path in order to keep the images uniformly distributed along it, while the NEB connects the images with imaginary springs and keeps them approximately uniformly distributed at all times due to the spring forces projected onto the direction of the path. Below we discuss the string method in details. I am referring the reader to Ref. [25] to learn more about the NEB.

The string method was used to obtain the Minimum Energy Paths in Fig. 2 connecting all neighboring minima of the 7-well potential using the Matlab code `string_7well.m`. The code `NEB_demo_2well.m` is a demo code implementing the NEB on a 2D two-well potential.

3.1. **Terminology.** For the further discussion, we will need the following terminology.

Definition 5. *Let $V(x)$, $x \in \mathbb{R}^n$, be a twice continuously differentiable function. Along with V, we consider the gradient $\nabla V(x)$ and the Hessian matrix*

$$H(x) := \left(\frac{\partial^2 V(x)}{\partial x_i \partial x_j} \right)_{i,j=1}^n .$$

- *A point $x_\star$ is **a stationary point** of $V(x)$ if $\nabla V(x_\star) = 0$.*
- *A stationary point $x_\star$ is **nondegenerate** if $H(x_\star)$ is full rank, or, equivalently, has no zero eigenvalues.*
- *The **Morse index** of a nondegenerate stationary point $x_\star$ is the number of of negative eigenvalues of the Hessian matrix $H(x_\star)$.*
- *A **Morse index one saddle** s is a nondegenerate stationary point of V such that the Hessian matrix $H(s)$ has a unique negative eigenvalue.*

3.2. **The string method.** The first version of the string method was proposed by E, Ren, and Vanden-Eijnden in 2002 [13]. An improved and simplified version was introduced by the same authors in 2007 [15]. An analysis of the curve evolution under the string method was conducted in [10]: it was shown how one can make up curves such that their evolution under the string method fails to converge to a MEP. These curves are quite fancy. Their failure to converge to a MEP is either linked to their special design and the presence of Morse index two stationary points. Stability and convergence to a MEP has been recently established in [37] provided that the initial path is close to this MEP, and this MEP passes through a sequence of m local minima, and each pair of minima in this sequence is separated by a single Morse index one saddle, $m \geq 2$.

3.2.1. *The curve evolution.* The string method is a numerical procedure accomplishing a curve evolution described below under the influence of a potential $V : \mathbb{R}^n \to \mathbb{R}$. A curve is a continuous image of a unit interval in $\mathbb{R}^n$. Moreover, the ends of the curve are fixed at two distinct critical points of the potential. Suppose the curve is differentiable and its configuration at time t is parametrized nondegenerately by $\alpha \in (A(t), B(t))$, i.e., the curve at time t is $\{\phi(\alpha, t) \mid \alpha \in (A(t), B(t))\}$ and its unit tangent vector is $\hat{\tau}(\alpha, t) = \frac{\phi_\alpha}{|\phi_\alpha|}$. Then the string method evolves it so that the normal velocity is the component of ∇V normal to the curve:

$$(40) \qquad \phi_t(\alpha, t) = -\nabla V^\perp(\phi(\alpha, t)) + \lambda \hat{\tau},$$

where

$$(41) \qquad \nabla V^\perp = \nabla V(\phi(\alpha, t)) - (\nabla V(\phi(\alpha, t)) \cdot \hat{\tau}(\alpha, t)) \, \hat{\tau}(\alpha, t).$$

The evolution of the curve is well defined, although $\lambda = \lambda(\alpha, t)$ is not unique. Different choices of λ correspond to different parametrizations. This is easy to see using the chain rule: if $\phi(\alpha, t)$ and $\tilde{\phi}(\tilde{\alpha}, t)$ represent the same evolving curve, then $\phi(\alpha, t) = \tilde{\phi}(\tilde{\alpha}(\alpha, t), t)$ and the differentiation gives

$$\phi_t = \tilde{\phi}_t + \tilde{\phi}_{\tilde{\alpha}}\tilde{\alpha}_t = \tilde{\phi}_t + \mu\hat{\tau} \text{ with } \mu = |\tilde{\phi}_{\tilde{\alpha}}|\tilde{\alpha}_t.$$

It is often convenient to choose a particular parametrization. For a robust numerical solution, a good choice is the unit-speed parametrization, i.e., $|\phi_\alpha| = 1$. Then $\lambda(\alpha, t)$ is fully determined, and α ranges over $(0, l(t))$ where $l(t)$ is the length of the curve at time t. Moreover, it is advantageous to avoid evaluation of $\nabla V^\perp$ [15]. If we set

$$\beta = \lambda + \left(\nabla V(\phi(\alpha, t)) \cdot \hat{\tau}(\alpha, t)\right),$$

then the evolution law is given by

(42) $$\phi_t(\alpha, t) = -\nabla V(\phi(\alpha, t)) + \beta(\alpha, t)\hat{\tau},$$

where $\beta(\alpha, t)$ is again uniquely determined by the requirement that $|\phi_\alpha| = 1$. To be stationary under Eqs. (40) or (42), a curve must satisfy $\nabla V^\perp(\phi) = 0$ pointwise. When this happens, Eq. (40) says that ϕ_t is everywhere tangent to the curve. Therefore, its image (as a geometric curve) does not change, although the parametrization may change in time. Thus: a piecewise smooth curve passing through a sequence of critical points x_1, ... , x_N (the points where $\nabla V(x) = 0$) is a stationary state of the string method if the curve is everywhere tangent to ∇V. Put differently: the curve is stationary if it consists of a sequence of critical points connected by heteroclinic orbits (solutions of $\dot{x} = -\nabla V(x)$ traced forward or backward in time). As noted previously, such curves are called Minimum Energy Paths.

3.2.2. *Numerical implementation.* Let x_A and x_B be two potential minima or two points lying close to two isolated potential minima. Let $\phi_0(\alpha)$, $\alpha \in [0, 1]$, be an initial curve connecting x_A and x_B, i.e., $\phi_0(0) = x_A$, $\phi_0(1) = x_B$. For example, $\phi_0(\alpha)$ can be a segment of straight line connecting x_A and x_B. We discretize the curve, i.e., represent it as a sequence of N points (these points are called "images" by chemical physicists)

$$\{\phi(\alpha_j)\}_{j=1}^N =: \{\phi_j\}_{j=1}^N, \quad \alpha_j = \frac{j}{N-1}.$$

Each iteration of the string method evolving a curve ϕ according to Eq. (42) consists of two substeps. Pick a time step h.

Gradient descent: Move images according to the gradient descent

$$\phi_j^* = \phi_j - h\nabla V(\phi_j), \quad 1 \le j \le N.$$

Reparametrization: Define a new continuous curve ϕ^* by interpolation between the updated images $\{\phi_j^*\}_{j=1}^N$. Distribute the new images ϕ_j^{new} uniformly along the curve ϕ^*.

Stop if the curve almost stops moving, i.e. if $\max_{1 \leq j \leq N} \|\phi_j^{new} - \phi_j\| < tol$ where tol is the user-prescribed tolerance.

Below is a Matlab code that does reparametrization:

```
function [x,l] = reparametrization(x)
% x is an n by d array. Row i of x is the i-th image along the path
% returns a uniformly reparametrized path and its length l
t = linspace(0,1,size(x,1));
dx = zeros(size(x));
dx = x - circshift(x,[1,0]);
dx(1,:) = zeros(1,size(x,2));
lxy = cumsum(sqrt(sum(dx.^2,2)));
l = lxy(end);
x = interp1(lxy/l,x,t);
end
```

3.3. **String method for SPDEs. Stochastic Allen-Cahn model.** An important advantage of path-based methods such as the string method is that they are applicable to high-dimensional SDEs and even to SPDEs. To illustrate this, we consider a well-known example of the Allen-Cahn PDE perturbed by white noise and find a transition path between its stable stationary solutions.

3.3.1. *Analysis of the Allen-Cahn PDE with periodic boundary conditions.* Allen-Cahn PDE (1979) [1] is a model for magnetization in alloys:

$$(43) \qquad\qquad u_t = \kappa \Delta u + u - u^3.$$

Let us consider PDE (43) in a 2D domain $\Omega = [0,1]^2$ with periodic boundary conditions, i.e.,

$$u(0,y) = u(1,y), \quad u_x(0,y) = u_x(1,y), \quad u(x,0) = u(x,1), \quad u_y(x,0) = u_y(x,1).$$

In this case, Eq. (43) has three uniform stationary solutions: $u \equiv 0$ is unstable, while $u \equiv 1$ and $u \equiv -1$ are stable (see the note of Trefethen [36] for more details). If κ is small enough, there also exist nonuniform stationary solutions, and their number increases as κ decreases [35] . The stability of stationary solutions can be assessed by considering the energy functional for Eq. (43) defined by

$$(44) \qquad\qquad V[u] := \int_\Omega \left[\frac{\kappa}{2} \left(u_x^2 + u_y^2 \right) + \frac{1}{4} \left(1 - u^2 \right)^2 \right] dxdy.$$

Let us find out how the energy functional will change if we add a perturbation δu also satisfying periodic boundary conditions to u (see the discussion in [35]). Hence, we consider

the difference $V[u + \delta u] - V[u] =$

$$= \int_\Omega \left[\frac{\kappa}{2} \left((u_x + \delta u_x)^2 + (u_y + \delta u_y)^2 \right) + \frac{1}{4} \left(1 - (u + \delta u)^2 \right)^2 \right] dxdy - V[u]$$

$$= \int_\Omega \left[\frac{\kappa}{2} \left((u_x)^2 + (u_y)^2 \right) + \kappa (u_x \delta u_x + u_y \delta u_y) + \frac{\kappa}{2} \left((\delta u_x)^2 + (\delta u_y)^2 \right) \right.$$

$$\left. + \frac{1}{4} \left(1 - u^2 \right)^2 - (1 - u^2) u \delta u + u^2 (\delta u)^2 - \frac{1}{2}(1 - u^2)\delta u^2 + O\left((\delta u)^3 \right) \right] dxdy - V[u].$$

Integrating by parts the terms with the first derivatives of δu we obtain:

$$V[u + \delta u] - V[u] = \int_\Omega - \left[\kappa(u_{xx} + u_{yy}) + u - u^3 \right] \delta u \, dxdy$$

$$+ \int_\Omega \left[\frac{\kappa}{2} \left((\delta u_x)^2 + (\delta u_y)^2 \right) + \frac{1}{2} \left(3u^2 - 1 \right) (\delta u)^2 \right] dxdy + O\left((\delta u)^3 \right)$$

(45)
$$:= I_1 + I_2 + O\left((\delta u)^3 \right).$$

The integral I_1 above shows that u is a stationary point of the energy functional if and only if $\kappa(u_{xx} + u_{yy}) + u - u^3 = 0$, i.e., u is a stationary solution of PDE (43). Indeed, otherwise, we can find δu such that the change in $V[u]$ due to perturbing u will be of the order of δu. A stationary point of a functional is called an *extremal*. In general, the function appearing in I_1 that is multiplied by δu, which is $- \left[\kappa(u_{xx} + u_{yy}) + u - u^3 \right]$ in this example, is called *the functional derivative* of $V[u]$ and denoted by $\frac{\delta V}{\delta u}$. The integral I_2 above shows that u is a minimizer of $V[u]$ if $u \equiv 1$ or $u \equiv -1$ as then the integrand is positive meaning that any perturbation δu leads to an increase of $V[u]$. On the other hand, if $u \equiv 0$, then the integrand is negative. Therefore, $u \equiv 0$ is an unstable stationary point of the energy functional.

In order to relate our conclusions regarding the extremals of the energy functional to the stability of the stationary solutions of the Allen-Cahn PDE, we determine how the energy functional changes along its solutions:

$$V[u(\cdot, t + dt)] - V[u(\cdot, t)] = V[u(\cdot, t) + u_t dt + O(dt^2))] - V[u(\cdot, t)]$$

$$= \int_\Omega - \left[\kappa(u_{xx} + u_{yy}) + u - u^3 \right] u_t dt dxdy + O(dt^2)$$

(46)
$$= - \left[\int_\Omega \left[\kappa(u_{xx} + u_{yy}) + u - u^3 \right]^2 dxdy \right] dt + O(dt^2) \leq 0.$$

Therefore, the energy functional is decreasing along all nonstationary solutions of PDE (43). Hence, $u \equiv 1$ and $u \equiv -1$ are stable stationary solutions, while $u \equiv 0$ is an unstable stationary solution of PDE (43).

With the notation $\frac{\delta V}{\delta u}$, one can write the Allen-Cahn PDE (43) in the form of a gradient descend in the functional space:

(47)
$$u_t = \kappa \Delta u + u - u^3 \equiv -\frac{\delta V[u]}{\delta u}.$$

3.3.2. *The Allen-Cahn PDE with frustrated boundary conditions.* Next, we consider the Dirichlet boundary conditions (BC) for PDE (43) given by

$$
(48) \qquad
\begin{cases}
u(0,y) = u(1,y) = 1, & 0 < y < 1, \\
u(x,0) = u(x,1) = -1, & 0 < x < 1, \\
u(0,0) = u(0,1) = u(1,0) = u(1,1) = 0.
\end{cases}
$$

With these boundary conditions, PDE (43) no longer has stable stationary solutions $u \equiv 1$ and $u \equiv -1$. If κ is small enough, it has stable stationary solutions close to those two. These stationary solutions for $\kappa = 0.005$ are plotted in Fig. 4. These solutions were
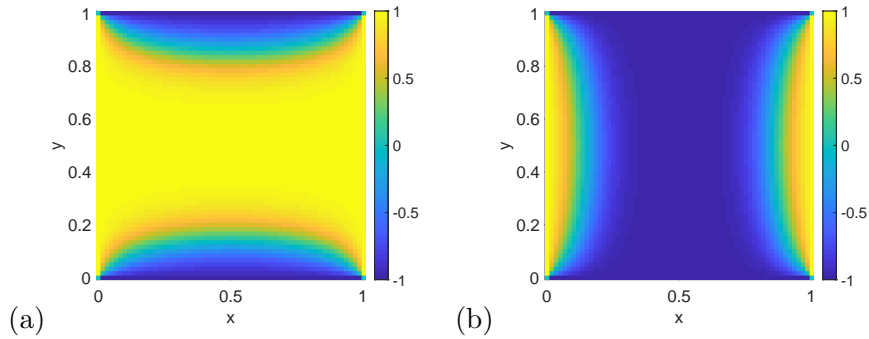

FIGURE 4. Stationary solutions to the Allen-Cahn PDE (43) with $\kappa = 0.005$ and boundary conditions (48).

found in MATLAB using the function `fsolve` applied to the system of nonlinear equations obtained via the standard finite-difference discretization of the Laplacian operator (see the code `AllenCahnString.m`). One can conduct stability analysis of solutions of PDE (43) with BC (48) as in was done for the case of periodic BC. The differences will be that (*i*) the perturbation δu must satisfy the homogeneous Dirichlet BC, i.e., $\delta u|_{\delta \Omega} = 0$, and (*ii*) stationary solutions will be different, in particular those shown in Fig. 4.

3.3.3. *Finding a transition path using the string method.* Now we perturb the Allen-Cahn PDE by white noise and obtain the following SPDE:

$$
(49) \qquad u_t = \kappa \Delta u + u - u^3 + \sqrt{\epsilon}\eta(x,y,t),
$$

where ϵ is a small parameter and η is the white noise satisfying

$$
E[\eta(x,y,t)\eta(x',y',t')] = \delta(x-x')\delta(y-y')\delta(t-t').
$$

We set $\kappa = 0.005$ and BC (48). Our goal is to find the maximum likelihood transition path between the two stable stationary solutions in Fig. 4. We will refer to them as u_1 adn u_{-1} respectively. Eq. (47) motivates the application of the string method for this purpose. Discretizing the Laplacian using finite differences, we reduce PDE (43) to a system of ODEs. Then the application of the string method is straightforward (see `AllenCahnString.m`).

The initial guess for the transition path obtained using linear interpolation between u_1 and u_{-1} is shown in Fig, 5(a). The final path is displayed in Fig. 5(b). The energy functional along the final path is plotted in Fig. 6.
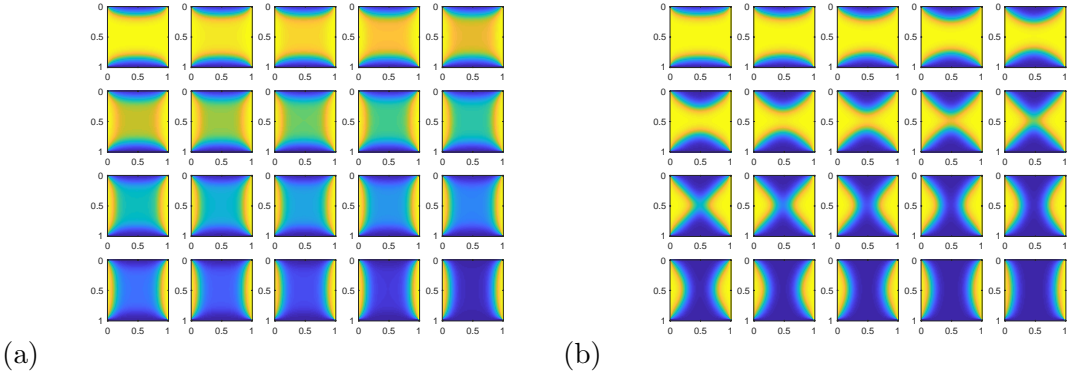

(a)

(b)

FIGURE 5. (a): The initial guess for the transition path between the two stable stationary solutions of the Allen-Cahn PDE in Fig. 4. (b):The transition path between them found by the string method. The colormap is the same as in Fig. 4.
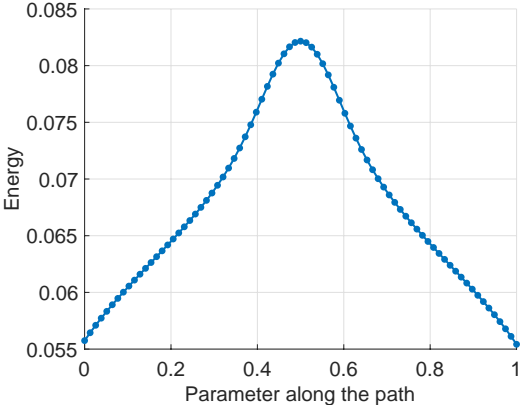

FIGURE 6. The energy functional along the path in Fig. 5(b).

Remark   • I would like to emphasize that there is no guarantee that the path found by the string method is the Maximum Likelihood Path. The output of the string method is biased by the initial guess. A visual example of this phenomenon is found in [13] where the string method has been originally presented. It is applied there to a bit different SPDE describing magnetization of a 2D plate. The two different

found paths presented there resulted from different initial guesses for the transition path. The energy graphs show that one of them is much more favorable than the other one.

- The string method is designed to evolve the path in such a manner that the maximal energy along it is nonincreasing. In contrast, the GMAM discussed in Section 5 applied to a gradient SDE does not have this important feature. One can design an example where the maximal energy increases as the path is evolved by the GMAM.

4. Methods for finding saddles

Once a MEP connecting two local minima of the given potential $V(x)$ is computed, one can find the images at which $V(x)$ along the MEP reaches local maxima. Typically, these images are close enough to Morse index one saddles and can serve for initialization of saddle finders.

Methods for finding saddles can be divided into three groups: one-image methods, two-image methods, and path-based methods. One-image methods are presented by the first saddle finder (to the best of my knowledge) proposed by Cerjan and Miller (1981) [7], its adjustment by Wales (1989) for finding saddles in energy landscapes of atomic clusters [38], and more recent development, the so-called *gentlest ascend dynamics* (GAD) by Gao, Leng, and Zhou [17, 18]. A simple and robust two-image method called the *dimer method* was proposed by Henkelman and Jonsson (1999) [21]. Later, Du and Zhang (2012) modified it into the *shrinking dimer method* and analyzed its dynamics and convergence properties [40]. We will consider the shrinking dimer method in details below. Ren and Vanden-Eijnden (2013) adjusted the string method for finding saddles adjacent to a given local minimum and called the resulting path-based method the *climbing string method* [30].

4.1. **The shrinking dimer method.** Here I present the basic version of the shrinking dimer method [40].

4.1.1. *Shrinking dimer dynamics.* A dimer is a line segment connecting a pair of points $x_1, x_2 \in \mathbb{R}^n$. Its length is

$$l = \|x_2 - x_1\|.$$

Its center is the point

$$x := \frac{x_1 + x_2}{2}.$$

Its direction is characterized by the unit vector

$$v := \frac{x_2 - x_1}{l}.$$

Given the position of the center x and the direction v one can restore the positions of the endpoints of the dimer:

$$x_1 = x - \frac{l}{2}v, \quad x_2 = x + \frac{l}{2}v.$$

The shrinking dimer dynamics is designed so that if the initial approximation is good enough, the dimer gets oriented so that the vector v is parallel to the eigenvector corresponding to the only negative eigenvalue, climbs to the saddle along the direction of this eigenvector (this is the gentlest ascend direction), and shrinks to a point while approaching the saddle.

Let $F_1 = -\nabla V(x_1)$ and $F_2 = -\nabla V(x_2)$ be the forces acting on the ends of the dimer. The force acting on the center of the dimer, F is defined as the average of these forces:

$$F = \frac{F_1 + F_2}{2}.$$

The difference of the forces acting on x_1 and x_2 is

$$\Delta F := F_2 - F_1.$$

The time evolution of the dimer is defined by the following system of ODEs:

$$(50) \qquad\qquad\qquad \mu_1 \dot{x} = (I - 2vv^T)F,$$

$$(51) \qquad\qquad\qquad \mu_2 \dot{v} = (I - vv^T)\Delta F/l,$$

$$(52) \qquad\qquad\qquad \mu_3 \dot{l} = -l.$$

The coefficients μ_1, μ_2 and μ_3 allow us to adjust the relationships between the speed of the motion of the center of the dimer, the speed of its rotation, and the speed of its shrinking.

The operator $(I - 2vv^T)$ in Eq. (50) reflects the vector F with respect to the hyperplane orthogonal to the unit vector v along the direction of the dimer. Note that F is parallel to v then

$$(I - 2vv^T)F = (I - 2vv^T)(-|F|v) = v|F| = -F,$$

If, in addition, v is parallel to the eigenvector u corresponding to the only negative eigenvalue of the Hessian matrix of the potential V, then the dimer moves directly uphill toward the saddle.

The operator $(I - vv^T)$ in Eq. (51) subtracts from the vector ΔF its component parallel to the direction of the dimer v. Hence $\dot{v}$ is orthogonal to v at all times. Therefore, the unit length of v is preserved.

The right-hand side of Eq. (52) is completely determined by l. Here we have picked the exponential shrinking law. One can pick another law.

The global convergence of the shrinking dimer method was proven in [40] for the quadratic potential of the form

$$V(z) = -\frac{z_1^2}{2} + \frac{1}{2}\sum_{i=2}^{n} z_i^2.$$

Precisely, for any initial condition x_0, $v_0 \in \mathbb{R}^n$ such that v_0 is not perpendicular to the vector $(1, 0, ..., 0)$, the solution of Eqs. (50)-(52) given by (2.4) will converge to (x^*, v^*, l^*) as $t \to \infty$, where $x^* = (0, ..., 0)$, $v^* = (1, 0, ..., 0)$ or $v^* = -(1, 0, ..., 0)$, and $l^* = 0$.

4.1.2. *Numerical implementation.* Pick a time step h. Pick the initial position of the center x_0, the initial direction of the dimer v_0, and the initial length l_0. Then for $k = 0, 1, 2, \ldots$ iterate:

$$(53) \qquad F_1 = -\nabla V(x_k - lv_k/2), \quad F_2 = -\nabla V(x_k + lv_k/2),$$

$$(54) \qquad F = \frac{1}{2}(F_1 + F_2), \quad \Delta F = F_2 - F_1,$$

$$(55) \qquad x_{k+1} = x_k + \frac{h}{\mu_1}(I - 2v_k v_k^T)F,$$

$$(56) \qquad w = v_k + \frac{h}{\mu_2 l_k}(I - v_k v_k^T)\Delta F,$$

$$(57) \qquad v_{k+1} = \frac{w}{\|w\|},$$

$$(58) \qquad l_{k+1} = \frac{l_k}{1 + h/\mu_3}.$$

This scheme is referred to as the Modified Euler scheme in [40]. The first two equations perform Forward Euler steps. Then v is normalized. l is updated according to the Backward Euler scheme. As a stopping criterion, you can use, for example, $|\nabla V(x)| < tol$ where tol is some reasonable tolerance.

Time evolution of the shrinking dimer method is illustrated in Fig. 7

The code `dimer_demo.m` uses the string method to find approximate locations of saddles and then the shrinking dimer method to nail down the locations of the saddles in a 2D three-well potential. The code `dimer_demo1.m` runs the dimer method starting from a uniform set of locations in the computational domain set up for the same 2D three-well potential.

5. Methods for finding Minimum Action Paths

Now we consider a system evolving according to

$$dx = b(x)dt + \sqrt{\epsilon}dw.$$

As it was pointed out in Section 1.7, the maximum likelihood transition path (a.k.a minimum action path (MAP) or instanton) from an attractor A_1 to an attractor $A2$ separated by a single transition state follows the rotational component of b but goes agains its potential component while going out of the basin of A_1 and then follows a trajectory to A_2.

If the quasipotential is computed, one is guaranteed to find the MAP (the global minimizer of the geometric action) by integrating the path

$$\psi_s = -\frac{b(\psi) + \nabla U(\psi)}{\|b(\psi) + \nabla U(\psi)\|}, \quad x \in \mathbb{R}^d$$
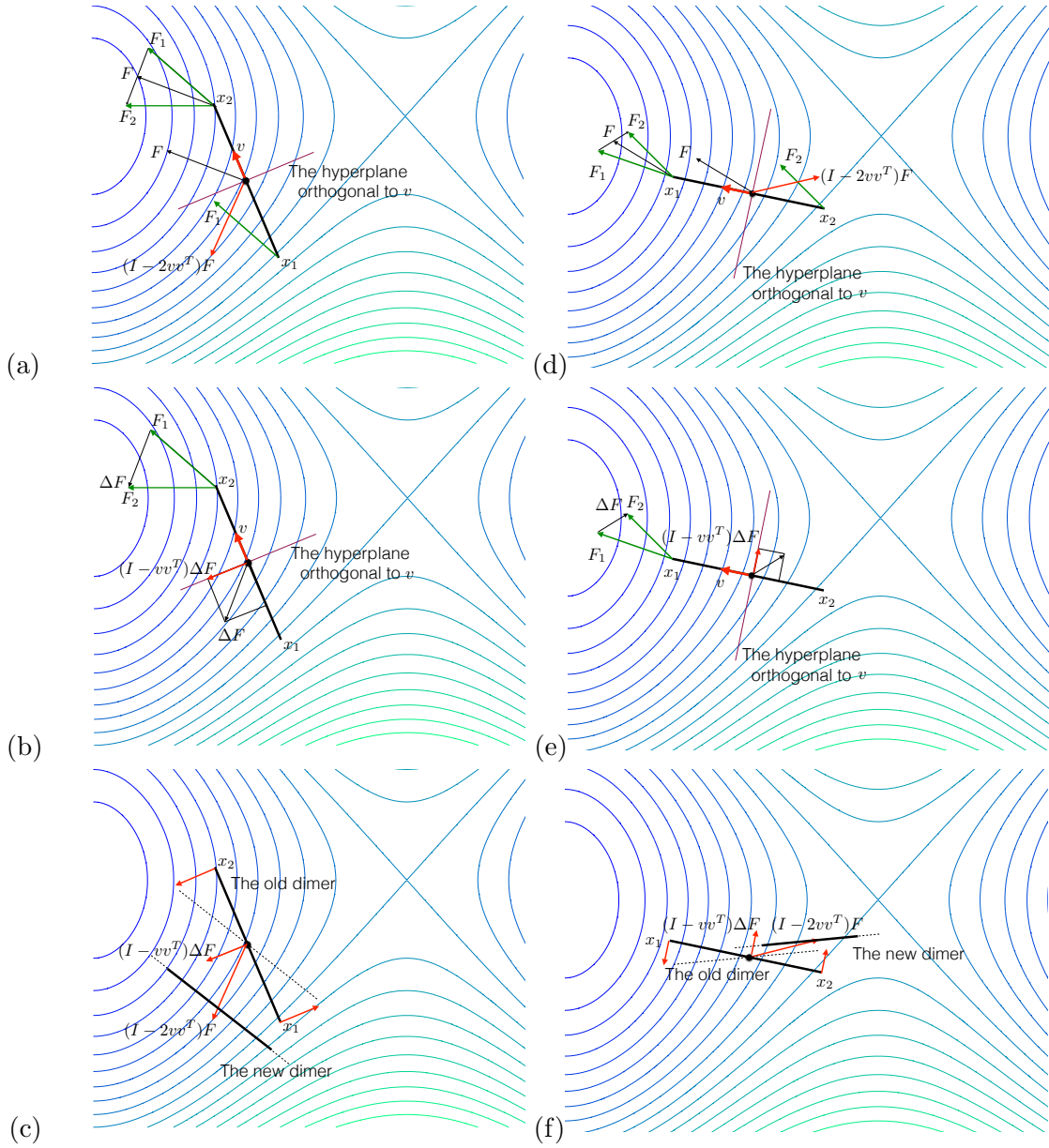
(a)

(b)

(c)

(d)

(e)

(f)

FIGURE 7. Illustration of one step of the shrinking dimer method on two examples of dimer. (a), (b), (c) : Example 1. (d), (e), (f): Example 2. (a), (c): Calculation of the vector $(I - 2vv^T)F$. (b), (e): Calculation of the vector $(I - vv^T)\Delta F$. (c), (f): The updated dimers.

starting from the found transition state that can be a saddle point, an unstable limit cycle, etc, .to the attractor, i.e., backwards. Currently, this approach is feasible in 2D and 3D [5, 8, 9, 39].

Alternatively, one can find the MAP using a path-based method, i.e., by solving a minimization problem in the space of curves. The advantage of path-based methods is that they work in any dimension and are simple-to-program in comparison with quasipotential solvers. Their shortcoming is that they are not guaranteed to find the global minimizer. Their outputs are biased to the initial guesses and can be local but not global minimizers, or merely extremal of the Freidlin-Wentzell or the geometric action.

To the best of my knowledge, the first proposed method for finding MAPs is the Minimum Action Method (MAM) by E, Ren, and Vanden-Eijnden (2004) [14]. The further developments in this direction resulted in the Geometric Minimum Action Method (GMAM) by Heymann and Vanden-Eijnden [22, 23] and in the Adaptive Minimum Action Method (AMAM) by Zhou, Ren, and E [41, 42]. The GMAM and the AMAM are based on a numerical minimization of the geometric action and the Freidlin-Wentzell action respectively. The GMAM is simpler, while the AMAM demonstrates a superior performance on systems such Lorenz'63 where the MAPs are complicated [42]. Below we consider the GMAM in more detail.

5.1. **Geometric Minimum Action Method.** A clear, concise, and straight-to-the-point presentation of the GMAM is given in [22]. Here I will provide some details that are omitted there. As we have shown in Section 1.4, the minimum action path (MAP) minimizes the geometric action

$$(59) \qquad S(\psi) = \int_0^1 \|\psi_\alpha\| \|b(\psi)\| - \psi_\alpha \cdot b(\psi) d\alpha, \quad \psi(0) = x_0, \ \psi(1) = x_1.$$

The GMAM is designed for finding MAPs between two asymptotically stable equilibria. An adjustment where one of the attractors is a limit cycle was recently proposed in [26]. In order to minimize the geometric action, we use *calculus of variation* in a similar manner as we did in Section 3.3.1.

Let ψ be a path satisfying the boundary conditions (BC) $\psi(0) = x_0$, $\psi(1) = x_1$, and let $\delta\psi$ be a small continuously differentiable perturbation of the path such that $\psi + \delta\psi$ also satisfies the same BC. Hence $\delta\psi(0) = 0$, $\delta\psi(1) = 0$. We consider the change in $S(\psi)$ occurring if ψ is perturbed by $\delta\psi$: $S(\psi + \delta\psi) - S(\psi)$. This can be done in a more general form for a functional of the form

$$S(\psi) = \int_0^1 L(\psi, \psi_\alpha) d\alpha.$$

Using the Taylor expansion, we calculate:

$$S(\psi + \delta\psi) - S(\psi) = \int_0^1 L(\psi + \delta\psi, \psi_\alpha + \delta\psi_\alpha) \, d\alpha - \int_0^1 L(\psi, \psi_\alpha) d\alpha$$

$$= \int_0^1 \left[\frac{\partial L}{\partial \psi} \delta\psi + \frac{\partial L}{\partial \psi_\alpha} \delta\psi_\alpha \right] d\alpha + O(\delta\psi^2) + O(\delta\psi_\alpha^2).$$

Integrating the term $\frac{\partial L}{\partial \psi_\alpha} \delta \psi_\alpha$ by parts and taking into account that $\delta \psi(0) = 0$, $\delta \psi(1) = 0$, we get:

$$(60) \qquad S(\psi + \delta \psi) - S(\psi) = \int_0^1 \left[\frac{\partial L}{\partial \psi} - \frac{d}{d\alpha} \frac{\partial L}{\partial \psi_\alpha} \right] \delta \psi \, d\alpha + O(\delta \psi^2) + O(\delta \psi_\alpha^2).$$

Eq. (60) shows that the path ψ is a local minimizer of $S(\psi)$ if and only if the following two conditions hold.

(1) The function in the square brackets in (60) is zero. This function is denoted by $\frac{\delta S}{\delta \psi}$ and called the *functional derivative*. The condition that it must be zero results in the famous *Euler-Lagrange equation*:

$$(61) \qquad \boxed{\frac{\delta S}{\delta \psi} := \frac{\partial L}{\partial \psi} - \frac{d}{d\alpha} \frac{\partial L}{\partial \psi_\alpha} = 0.}$$

Otherwise, we can find a perturbation $\delta \psi$ that decreases $S(\psi)$.

(2) The term $O(\delta \psi^2) + O(\delta \psi_\alpha^2)$ must be positive unless $\delta \psi \equiv 0$. In order to check this condition, one needs to Taylor-expand the integrand in $S(\phi)$ further as it was done in Section 3.3.1.

If the path ψ satisfies the Euler-Lagrange equation (61), ψ is called an *extremal* of $S(\psi)$. It might be a local minimizer, a local maximizer, or neither. Even if both conditions hold, we can only say that ψ is a local minimizer of $S(\psi)$, while the MAP must be the global minimizer.

The GMAM is based on a numerical solution of the Euler-Lagrange equation for the geometric action (59). Hence, even if it properly converges, the only guarantee that can be given is that the resulting path approximates an extremal of $S(\psi)$.

Recall that the value of the geometric action (59) is independent of the parametrization of the path ψ. Therefore, the simplest possible parametrization is chosen for the GMAM: $\|\psi_\alpha\|$ is constant along the path and is equal to l, the length of ψ.

Substituting the integrand of the geometric action for L in the Euler-Lagrange equation (61) and applying the condition $\|\psi_\alpha\| = $ const, one obtains the following equation for an

extremal of $S(\psi)$ after a careful and tedious calculation:

$$(62) \qquad \lambda \frac{\delta S}{\delta \psi} = -\lambda^2 \psi_{\alpha\alpha} + \lambda \left(\nabla b - (\nabla b)^\top \right) \psi_\alpha + (\nabla b)^\top b - \lambda \lambda_\alpha \psi_\alpha, \quad \text{where}$$

$$\lambda := \frac{\|b\|}{\|\psi_\alpha\|},$$

$$\nabla b := \left(\frac{\partial b_i}{\partial x_j} \right) = \begin{bmatrix} \frac{\partial b_1}{\partial x_1} & \frac{\partial b_1}{\partial x_2} & \cdots \\ \frac{\partial b_2}{\partial x_1} & \frac{\partial b_2}{\partial x_2} & \cdots \\ \vdots & \vdots & \end{bmatrix},$$

$$\psi(\alpha) = \begin{bmatrix} x_1(\alpha) \\ x_2(\alpha) \\ \vdots \end{bmatrix}.$$

The GMAM proceeds as follows. First, we pick an initial guess for the path ψ. Often, it is a line segment connecting x_0 and x_1. Sometimes, as it is in the Maier-Stein system [28], the initial path being the line segment connecting its two asymptotically stable equilibria leads to a wrong result which can be identified, for example, by comparing values of $S(\psi)$ at outputs of the GMAM starting from a collection of various initial paths.

Next, we discretize the path into N points uniformly distributed along the path:

$$\{x_0 \equiv \psi_1, \psi_2, \ldots, \psi_{N-1}, \psi_N \equiv x_1\}.$$

The points ψ_1 and ψ_N remain fixed, while the points ψ_j, $j = 2, \ldots, N-1$, are evolved by the GMAM. Each step of the GMAM consists of two substeps: steepest descent and reparametrization.

Steepest descent. The following linearly-implicit scheme is implemented for the steepest descent step. This choice of the scheme allows us to use rather large time steps without creating stability problems. Let ψ_j be the jth point of the current path and $\tilde{\psi}_j$ be the jth point of the updated path. The function λ, the forcing b, and the tensor ∇b are evaluated at the current path ψ, while the second derivative of the path with respect to α is evaluated at the updated path $\tilde{\psi}$. Let τ be the time step and $h = (N-1)^{-1}$ be the step in α. Then

$$\frac{\tilde{\psi}_j - \psi_j}{\tau} = \frac{(\lambda_j)^2}{h^2} \left[\tilde{\psi}_{j+1} - 2\tilde{\psi}_j + \tilde{\psi}_{j-1} \right]$$

$$- \lambda \left[\nabla b(\psi_j) - (\nabla b(\psi_j))^\top + \lambda_j \frac{\lambda_{j+1} - \lambda_{j-1}}{2h} \right] \frac{\psi_{j+1} - \psi_{j-1}}{2h}$$

$$(63) \qquad - (\nabla b(\psi_j))^\top b(\psi_j).$$

The implementational details of this scheme can be read off from my code `gmam.m` that finds a MAP in the Maier-Stein system [28].

Reparametrization. The points $\tilde{\psi}_j$ are not uniformly distributed along the path $\tilde{\psi}$ obtained as a result of one step of the linearly-implicit scheme (63). To maintain the rule $\|\psi_\alpha\| = \text{const}$ along the path at all times based on which Eq. (62) is derived, we

reparametrize $\tilde{\psi}$ and obtain the new path ψ. The reparametrization is performed in the same way as it is done in the string method. In `gmam.m`, this procedure is organized in a separate function within the file.

Remark
- The GMAM works very well in arbitrary dimensions, even for discretized SPDEs, where the transition paths are simple in the sense that they do not involve high-curvature segments. In particular, the endpoints should not be spiral points. If the path spirals, the path evolution by the GMAM slows down and a stopping criterion gets satisfied before the path converges to the spiraling part. In contrast, the AMAM is able to converge to spiraling paths as it is shown on the example on the Lorenz'63 system [42]
- A very important advantage of the GMAM is its relative simplicity: it is easy-to-program. Thanks to it, it has become quite popular.
- As we have discussed, one can only guarantee that the output of the GMAM approximates an extremal of the geometric action provided that the method has converged. An alternative approach based on computing the quasipotential on a mesh by Dijkstra-like algorithms has been developed in [5, 8, 9, 39]. Once the quasipotential is found, one can obtain the global minimizer of the geometric action by direct integration. However, this approach is currently developed for at most 3D SDEs and requires much more programming efforts. The first 2D quasipotential solver [5] has become the core for the R package `Qpot` that is publicly available on cran. A detailed description of this package in found in the R Journal (see Ref. [29]).

REFERENCES

[1] S. M. Allen and J. W. Cahn, A microscopic theory for antiphase boundary motion and its application to antiphase domain coarsening, Acta Metallurgica, **27**, 6 (1979), 1085–1095

[2] R. Bartels and G. W. Stewart, Solution of the matrix equation AX+ XB = C, Comm A.C.M., **15**, 9, 820–826 (1972)

[3] Bellman, R., Dynamic Programming, Princeton Press, New Jersey, 1957.

[4] F. Bouchet and J. Reygner, *Generalisation of the Eyring-Kramers Transition Rate Formula to Irreversible Diffusion Processes*, Annales Henri Poincare, 17 (2016), 12, pp. 3499–3532

[5] M. K. Cameron, Finding the Quasipotential for Nongradient SDE's, Physica D: Nonlinear Phenomena, 241 (2012), pp. 1532-155

[6] M. K. Cameron, Construction of the quasi-potential for linear SDEs using false quasi-potentials and a geometric recursion, arXiv:1801.00327 (2017)

[7] C. Cerjan and W. Miller, On finding transition states, The Journal of Chemical Physics 75, 2800 (1981)

[8] D. Dahiya and M. Cameron, Ordered Line Integral Methods for Computing the Quasi-potential, J. Sci. Comput. (2017), https://arxiv.org/pdf/1706.07509.pdf

[9] D. Dahiya and M. Cameron, An Ordered Line Integral Method for Computing the Quasi-potential in the case of Variable Anisotropic Diffusion, Physica D 382-383 (2018), 33–45, arXiv:1806.05321

[10] M. Cameron, R. Kohn, and E. Vanden-Eijnden, The String Method as a Dynamical System, Journal of Nonlinear Science, 21, Number 2, pp. 193-230 (2011)

[11] Z. Chen, M. Freidlin, *Smoluchowski-Kramers approximation and exit problems*, Stoch. Dyn. 5 (2005), 4, pp. 569–585

[12] Z. Chen, *Asymptotic Problems related to Smoluchowski-Kramers approximation*, Ph.D. Dissertation, UMD, 2006

[13] E, W., Ren, W., Vanden-Eijnden, E.: String method for study of rare events. Phys. Rev. B 66, 052301 (2002)

[14] W. E, W. Ren, and E. Vanden-Eijnden, Minimum Action Method for the Study of Rare Events, Comm. Pure Appl. Math., **57**, 0001–0020 (2004)

[15] E, W., Ren, W., Vanden-Eijnden, E.: Simplified and improved string method for computing the minimum energy paths in barrier-crossing events. J. Chem. Phys. 126, 164103 (2007)

[16] Freidlin, M. I. and Wentzell, A. D., Random Perturbations of Dynamical Systems, 2nd edition, Springer, New York, 1998, 3rd Edition, Springer, New York, 2013

[17] W. Gao, J. Leng, X. Zhou, An iterative minimization formulation for saddle point search, SIAM J. Numer. Anal. **53** 4, 1786–1805 (2015)

[18] W. Gao, J. Leng, X. Zhou, Iterative minimization algorithm for efficient calculations of transition states, J. Comp. Phys., **309** (2016) 69–87

[19] C. Gissinger, A new deterministic model for chaotic reversals Eur. Phys. J. B (2012) 85: 137. https://doi.org/10.1140/epjb/e2012-20799-5

[20] E. Heinz, *Beitr age zur St orungstheorie der Spektralzerlegung*, Math. Ann. 123 (1951) pp. 415-438.

[21] G. Henkelman and H. Jonsson, A dimer method for finding saddle points on high dimensional potential surfaces using only first derivatives, J. Chem. Phys., 111 (1999), pp. 7010–7022.

[22] Heymann, M. and Vanden-Eijnden, E., Pathways of maximum likelihood for rare events in non-equilibrium systems, Application to nucleation in the presence of shear, Phys. Rev. Letters **100** 14, 140601 (2008)

[23] Heymann, M. and Vanden-Eijnden, E., The Geometric Minimum Action Method: A Least Action Principle on the Space of Curves, Comm. Pure Appl. Math. **61**, 8, 1052-1117 (2008)

[24] W. Hurewicz, Lectures on ordinary differential equations, Dover Publications, New York, 1990 (based on lectures given by W. Hurewicz in 1943)

[25] Jonsson, H., Mills, G., Jacobsen, K.W.: Nudged elastic band method for finding minimum energy paths of transitions. In: Berne, B.J., Ciccoti, G., Coker, D.F. (eds.) Classical and Quantum Dynamics in Condensed Phase Simulations, p. 385. World Scientific, Singapore (1998)

[26] L. Lin, H. Yu, and X. Zhou, Quasi-potential Calculation and Minimum Action Method for Limit Cycle, J. Nonlin. Sci., **29**, 3 (2019), 961–991

[27] E. N. Lorenz, Deterministic Nonperiodic Flow, J. Atmospheric Sci., 20 (1963), 2 pp. 130–141

[28] R. S. Maier and D. L. Stein, A scaling theory of bifurcations in the symmetric weak-noise escape problem, J. Statist. Phys. **83**, no. 3-4, 291–357 (1996)

[29] C. Moore, C. Stieha, B. Nolting, M. Cameron, and K. Abbott, QPot: An R Package for Stochastic Differential Equation Quasi-Potential Analysis, The R Journal Vol. 8/2, December 2016

[30] W. Ren and E. Vanden-Eijnden, A climbing string method for saddle point search, J. Chem. Phys. 138, 134105 (2013)

[31] O. E. Roessler, An Equation for Continuous Chaos", Physics Letters, 57A (5): 397?398 (1976)

[32] J. .A. Sethian, A. Vladimirsky, Ordered Upwind Methods for static Hamilton-Jacobi-Bellman equations, Proc. Natl. Acad. Sci. 98 (2001)11069–11074

[33] J. A. Sethian, A. Vladimirsky, Ordered Upwind Methods for static Hamilton-Jacobi-Bellman equations: theory and algorithms, SIAM J. Numer. Anal. 41, 1 (2003) 325–363

[34] S. H. Strogatz, *Nonlinear dynamics and Chaos*, 2nd edition, Westview Press, 2015

[35] M. Tao, Hyperbolic periodic orbits in nongradient systems and small-noise-induced metastable transitions, Physica D **363** (2018) 0?16

[36] L. N. Trefethen, Allen-Cahn or bistable equation

[37] B. Van Koten and M. Luskin, Stability and convergence of the string method for computing minimum energy paths, arXiv:1807.06094, expected to come out in SIAM MMS

[38] D. Wales, Finding saddle points for clusters, J. Chern. Phys. **91** (11), 7002 (1989)

[39] S. Yang, S. Potter, and M. Cameron, Computing the quasipotential for nongradient SDEs in 3D, Journal of Computational Physics, 379 (2019) 325-350, https://doi.org/10.1016/j.jcp.2018.12.005, arXiv: 1808.00562

[40] J. Zhang, Q. Du, Shrinking dimer dynamics and its applications to saddle point search, SIAM J. Numer. Anal., **50**, 4, 1899-1921 (2012)

[41] X. Zhou, W. Ren, Weiqing, W. E, Adaptive minimum action method for the study of rare events, J. Chem. Phys. 128, 104111 (2008)

[42] X. Zhou, W. Ren, Weiqing, W. E, Study of noise-induced transitions in the Lorenz system using the minimum action method. Commun. Math. Sci. 8(2), 341–355 (2010)